

# Use of Catastrophe Theory to Establish Safety Assessment Model for Timber-Framed Heritage Buildings

Wei Qian,<sup>a,b,c</sup> ShuaiBing Li,<sup>a</sup> and Wei Wang<sup>a,b,c,\*</sup>

Catastrophe theory was used to establish a safety assessment model to reduce the reliance on subjective judgments in evaluation of timber-framed heritage buildings. This study was conducted in three phases. Initially, a comprehensive evaluation index system was established from the perspective of foundation. It consisted of eight aspects and 25 safety evaluation indicators using superstructure load-bearing elements, maintenance structures, and their interconnections in timber-framed heritage buildings. The 25 safety evaluation indicators included foundation, base, stone piers, columns, beams, lintels (beams, pads, and other bending components), bracket sets, arches, maintenance walls, beam-brace connections, and roof structures. The bottom-level indicators in the index system were dimensionless. The second phase employed typical catastrophe models (cusp, swallowtail, and butterfly) for normalization, resulting in calculated catastrophe scales and evaluation levels. The case study of the Buddha Hall of Zhihua Temple, Beijing, was applied in the final phase. It was found that the catastrophe scales method solved the subjectivity issues in determining weights. Additionally, the calculations were found to be concise and reliable, providing accurate results. The model can be used as a theoretical reference for the future safety assessment of timber-framed heritage buildings.

DOI: 10.15376/biores.19.3.6690-6710

*Keywords: Catastrophe theory; Timber structure; Heritage buildings; Safety assessment*

*Contact information: a: Faculty of Architecture, Civil and Transportation Engineering, Beijing University of Technology, Beijing 100124, China; b: Beijing Engineering Technology Research Center for Historic Building Protection, Beijing 100124, China; c: Key Science Research Base of Safety Assessment and Disaster Mitigation for Traditional Timber Structure (Beijing University of Technology), State Administration for Cultural Heritage, Beijing 100124, China; \*Corresponding author: ieeww@bjut.edu.cn*

## INTRODUCTION

Chinese architecture has an independent structural system. It has a long history and covers vast areas and regions of China. For thousands of years, although China has often been in contact with other countries in military and political aspects, the basic structure of architecture has not been affected by other influences and it still maintains its wooden structure. Chinese wooden structure building is not only the embodiment of the material form, but also carries the spiritual character and cultural gene characteristics of the Chinese nation, which has a very high historical, cultural and social value (Liang 2007). However, the safety protection of ancient buildings in China remains a concern. Many cultural heritage units are gradually deteriorating, and the damage to timber structures often goes unnoticed. Therefore, the safety identification and assessment of ancient buildings are crucial for preventive protection procedures.

The wooden structures are the main load-bearing system of timber-framed heritage buildings. Compared to modern buildings, heritage buildings have complex material properties and force systems, posing challenges and difficulties in safety assessment. Currently, evaluating approaches of the timber structures typically involve a combination of quantitative and qualitative methods. For instance, Cointe *et al.* (2007) used a method to assess the health of ancient wooden-framed structures based on field measurements and numerical coupling simulations. Garziera *et al.* (2025) utilized interferometric radar-based non-destructive testing to detect and evaluate the health conditions of ancient buildings. Lima *et al.* (2018) applied fiber optic grating sensors to monitor and assess the structural health of the Aviroda Church. In China, researchers have employed methods such as fuzzy comprehensive evaluation, grey system theory, neural network evaluation, and matter-element extension methods to investigate the safety assessment of timber-framed heritage buildings. However, these methods require the subjective determination of relevant indicator weights, influencing the objectivity of the assessment results. For example, Gu (2009) proposed a fuzzy comprehensive judgment theory for reliability assessment of brick and stone pagodas. Xu *et al.* (2017) applied analytic hierarchy process, grey fuzzy analysis, and grey whitening weight function to the safety assessment of wooden-framed heritage buildings. Additionally, fuzzy hierarchical analysis models and BP neural network models for the assessment of timber-framed heritage buildings have been used (Qin *et al.* 2017; Luo *et al.* 2020). Wang *et al.* (2022) applied the matter-element model to diagnose health and assess safety of ancient wooden structures, and Zhang *et al.* (2017) used an improved Elman neural network to predict the lifespan of ancient buildings. These methods mentioned above use subjective calculation of the weights.

Both Chinese and overseas researchers have applied catastrophe theory to research in various fields. For instance, Abrahamyan *et al.* (2023) applied catastrophe theory to voice quality research. Stamovlasis *et al.* (2022) utilized catastrophe theory in neuropsychological studies, exploring the nonlinear impact of depression on financial capacity in individuals with mild cognitive impairment and dementia. Another study employed catastrophe theory to establish a risk assessment model for sudden water and mud in karst tunnels (Zhu *et al.* 2020). The catastrophe theory was applied for predicting construction risks in subway stations (Jiang *et al.* 2020), to assess the danger of gas pipelines in collapsed mining areas (Shu *et al.* 2017), to assess the fire risk of high-rise civil buildings (Zeng 2021), to assess the safety risk of highway bridge construction (Li 2023), and to evaluate the fire hazard of ancient wooden structures (Gao *et al.* 2023). However, in the field of safety assessment of wood-framed ancient buildings, the application of catastrophe theory is not yet common. Changes in the safety of ancient buildings can be understood based on the changes in the various components within the building caused by the qualitative change of the system. The transition of the system from a safe state into a hazardous state can be regarded as a mutation phenomenon. Thus, the formation of the damage pathway in a wood-framed ancient building is also in line with the laws of catastrophe theory. Therefore, the safety assessment of wood-framed ancient buildings has certain compatibility with the catastrophe theory. In addition, the catastrophe theory also considers the relative importance of each evaluation index, and combines qualitative and quantitative, and mainly quantitative, which effectively reduces the interference of human factors on the results and makes the final results more objective. This study integrated catastrophe theory into comprehensive evaluation and established an index system for the safety assessment of timber-framed heritage buildings. Quantitative recursive operations

were performed based on normalization formulas, calculating the final catastrophe scale values for the safety level of timber-framed heritage buildings.

## EXPERIMENTAL

### Catastrophe Theory

The catastrophe theory was developed by René Thom, a French mathematician in the last century (Zhou 1989). It is a mathematical theory that investigates the discontinuous and sudden changes occurring in dynamic systems during continuous developmental processes, and the interweaving relationships with continuous factors of change. Many study subjects do not exhibit a continuous state but rather manifest a particular state abruptly at a critical point. Using the concepts from topological dynamics and singularity theory, catastrophe theory uses a potential function and characterizes the changing states of study subjects by establishing a potential function. This characterization process distinguishes the critical points at which the study subject undergoes a change. The theory then analyzes the discontinuous changes on either side of these critical points. Ultimately, the elementary catastrophe models are developed (Ling 1987).

Typically, the variables in the potential function are divided into two categories based on the different states by which they are characterized. The first category is the state variables, primarily representing the behavioral states of the study subject itself. The second category is the control variables, used to characterize the factors influencing the changes in the variables on either side. Assuming the potential function is denoted as  $f(x)$ , taking its derivative, and setting the 1<sup>st</sup> derivative  $f'(x) = 0$ , yields its equilibrium surface. Working for the odd points set of the equilibrium surface with the 2<sup>nd</sup> derivative  $f''(x) = 0$  gives the bifurcation equation with only the control variables. When the control variables change to align with the equation, it signifies the occurrence of a catastrophe in the study subject. It allows the identification of critical points for each control variable causing the catastrophe (Li *et al.* 2011). Table 1 presents four typical elementary catastrophe models with their corresponding formulaic expressions.

**Table 1.** Four Common Catastrophe Models (Kang 2014)

Mutation Model	Controlled Variables	State Variables	Potential Function	Bifurcation Equation
Folded Type	1	1	$f(x) = x^3+ax$	$a = 0$
Pointed Type	2	1	$f(x) = x^4+ax^2+bx$	$a = -6x^2, b = 8x^3$
Swallow-tail Type	3	1	$f(x) = x^5+ax^3+bx^2+cx$	$a = -6x^2, b = 8x^3, c = 3x^4$
Butterfly Type	4	1	$f(x) = x^5+ax^4+bx^3+cx^2+d$	$a = -10x^2, b = 20x^3, c = -15x^4, d = 4x^5$

Note: x and y are state variables, while a, b, c, and d are control variables

Table 1 presents commonly used catastrophe models through meticulous calculations. While the computational process is intricate, the processes are relatively straightforward. Taking the swallowtail catastrophe model as an example, the general expression for its potential function is  $f(x) = x^5+ax^3+bx^2+cx$ . Calculating its first and second derivatives results in  $df(x) = 5x^4+3ax^2+2bx+c$ ,  $d^2f(x) = 20x^3+6ax+2b$ , respectively. The

bifurcation equation is obtained by eliminating the equilibrium surface  $df(x) = 0$  and the odd points set  $d^2f(x) = 0$ .

From the bifurcation equations of the catastrophe models (see Table 1), the normalization equations for each model are developed. Given the various states of variables within the system, it is convenient to normalize the values of control and state variables to the range  $[0, 1]$ . This normalization process aligns with the principles of fuzzy membership functions, facilitating the direct calculation of the overall catastrophe membership function values using the provided formulas. Equations 1 to 4 below correspond to the normalization equations for the four common catastrophe models presented in Table 1.

For the fold catastrophe model:

$$x_a = a^{\frac{1}{2}} \quad (1)$$

For the cusp catastrophe model:

$$x_a = a^{\frac{1}{2}}, x_b = b^{\frac{1}{3}} \quad (2)$$

For the swallowtail catastrophe model:

$$x_a = a^{\frac{1}{2}}, x_b = b^{\frac{1}{3}}, x_c = c^{\frac{1}{4}} \quad (3)$$

For the butterfly catastrophe model:

$$x_a = a^{\frac{1}{2}}, x_b = b^{\frac{1}{3}}, x_c = c^{\frac{1}{4}}, x_d = d^{\frac{1}{5}} \quad (4)$$

Figure 1 shows schematic diagrams of the four common catastrophe models.

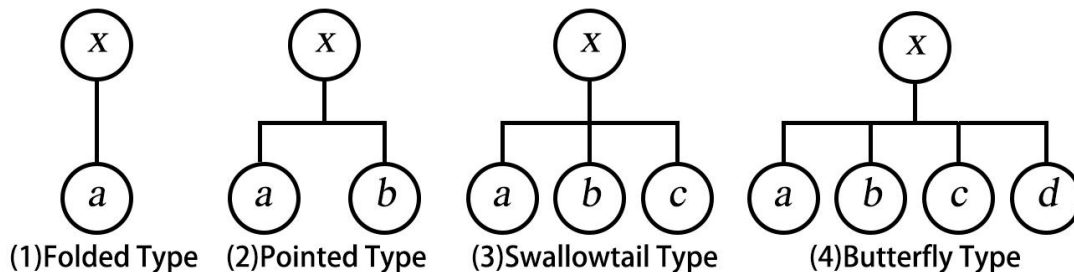


Fig. 1. Schematic diagram of four common mutation Model system

### The Process of Safety Assessment of Wood-framed Ancient Buildings

The flowchart of this study on the safety assessment of ancient wood-framed buildings is shown below (Fig. 2):

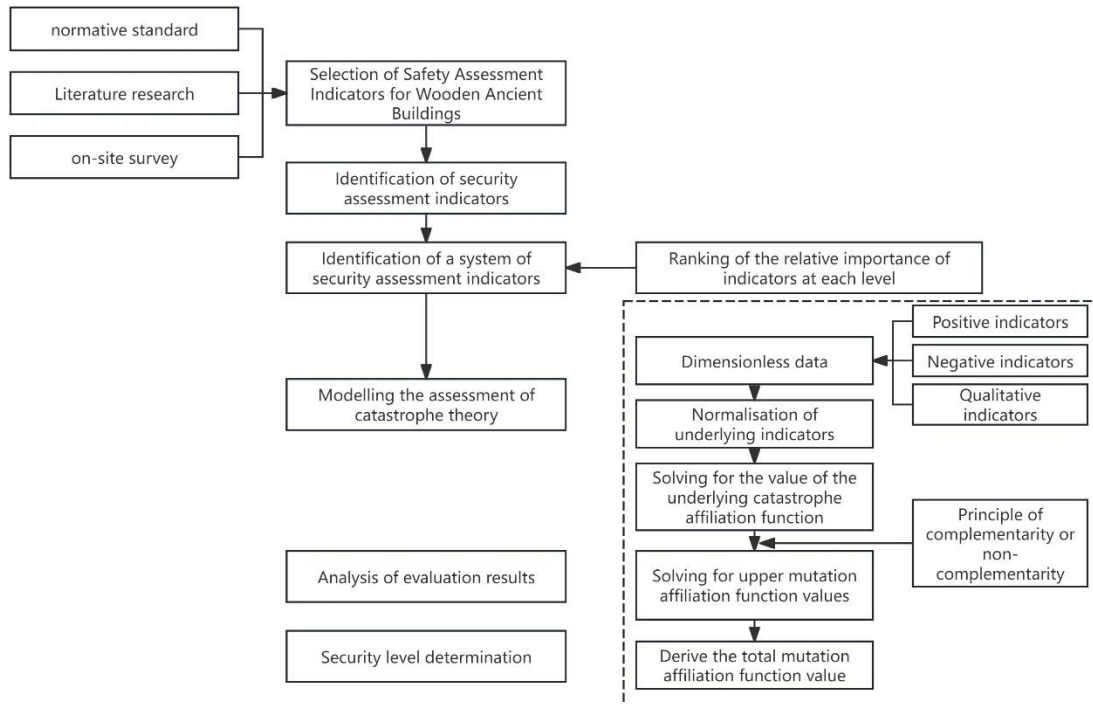


Fig. 2. The process of safety assessment of wood-framed ancient buildings

## Safety Assessment of Timber-Framed Heritage Buildings (Based on Catastrophe Theory)

### *Safety assessment index system for timber-framed heritage buildings*

The factors influencing the safety of wooden components in ancient buildings are numerous, encompassing both quantitative and qualitative aspects. These factors are not entirely independent, and they continuously interact with each other. Therefore, when selecting indicators, priority should be given to those that can reflect the maximum amount of information with the least number of measurements. The structural characteristics of wooden structures in ancient buildings are considered. Standards such as “Reliability appraisal standards for civil buildings,” (GB 50292 2015), “Seismic appraisal standards for buildings,” (GB 50023 2009), “Technical specifications for maintenance and strengthening of wooden structures in ancient buildings,” (GB 50165-92 1993), and relevant literature are incorporated (Ma 2007; Gu 2009, Pan *et al.* 2016; Huan *et al.* 2019; Wang 2020; Wang *et al.* 2022). Then, the evaluation is categorized into eight aspects: foundation, base and stone activities, columns, beams (lintels, pads, and other flexural members), bracket sets, maintenance walls, beam-frame associations, and roof structures. A total of 25 assessment indicators are selected to establish an evaluation index system for wooden structures in ancient buildings, as illustrated in Fig. 3.

### *Quantitative factor evaluation index grading standards*

Based on the varying levels of impact on safety, wooden structures in ancient buildings are classified into four categories (see Table 2), and the definitions of symbols in and Table 2 are explained (see Table 2.1). The standard for the evaluation indicators of safety factors in wooden structures of ancient buildings is used in this classification process.

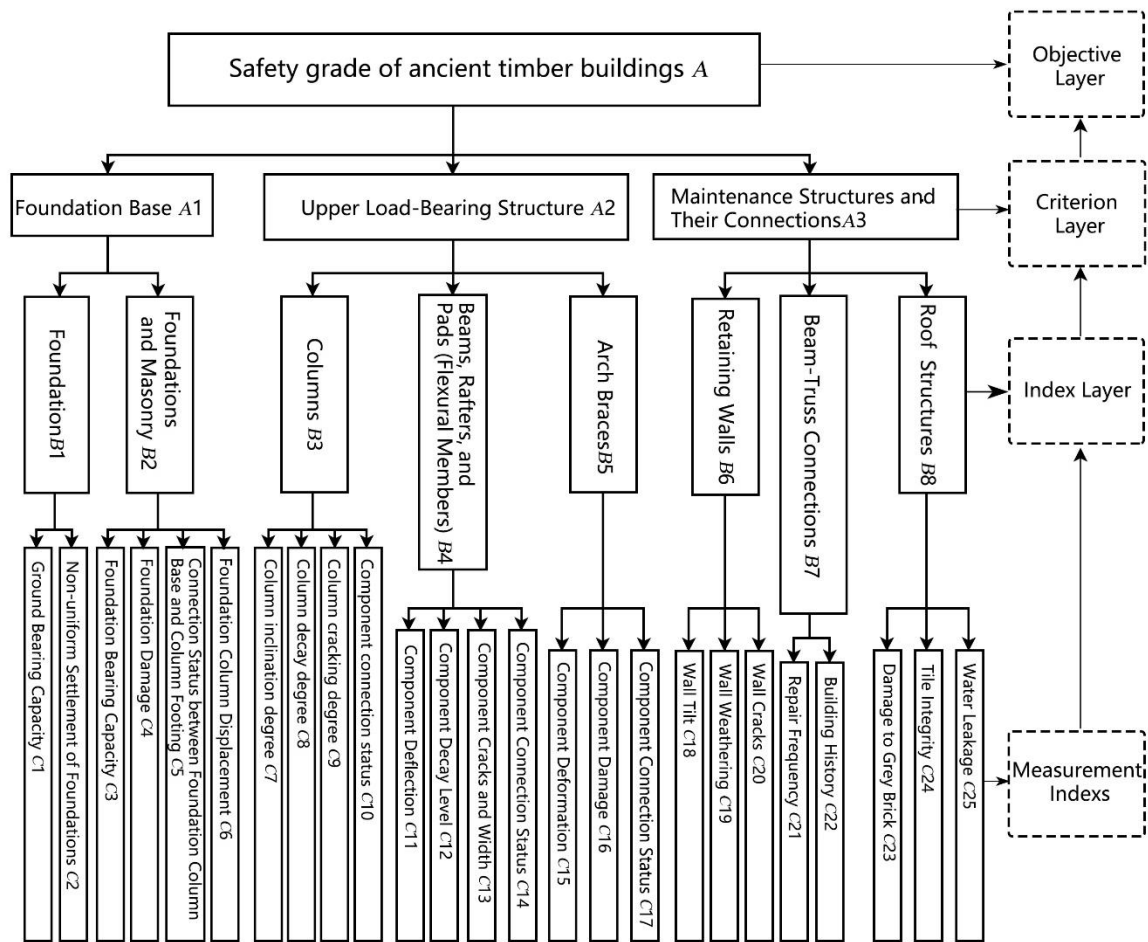


Fig. 3. Wood structure safety evaluation index system

Table 2. The Assessment Index Classification Standard for Qualitative Factors

	Evaluation Criteria	Safety Level I	Mild Hazard Level II	Moderate Hazard Level III	Severe Hazard Level IV
Column	Column inclination degree/mm	$\leq D/8$	$D/8$ to $D/4$	$D/4$ to $D/2$	$\geq D/2$
	Column decay degree	Surface Decay or Aging Deterioration; For $0 \leq \rho_1 < 1/10$ , no heart rot, no knots.	Surface decay or aging deterioration; For $1/10 \leq \rho_1 < 1/7$ , no heart rot; Knot size ratio $m < 1/5$ .	Surface decay or aging deterioration; For $1/7 \leq \rho_1 < 1/5$ , no heart rot; Knot diameter ratio $m < 1/5$ .	Surface decay and aging deterioration rate; $\rho_1 < 1/5$ or heart rot $\rho_1 > 1/7$ ; Critical stress location $m < 1/3$ .
	Column cracking degree	No continuous crack along any part of the column length; Maximum crack depth $< 0.5R$	No continuous crack along any part of the column length; Maximum	Continuous cracks along the column length; Maximum crack depth $0.5R$ .	Continuous cracks along the column length; Maximum crack depth $0.5R \sim R$ .

			crack depth 0.5R ~ R.		
	Component connection status( $s_1$ )	$< l_0/8$	$l_0/8$ to $l_0/4$	$l_0/4$ to $l_0/2$	$> l_0/2$
Foundation	Ground Bearing Capacity ( $P_{dmax} / (1.2f_{sc})$ )	$\geq 1.00$	1.00 to 0.95	0.95 to 0.90	$< 0.90$
	Non-uniform Settlement of Foundations/mm	Non-uniform settlement is less than the allowable settlement difference specified in the current national standard "Code for the Design of Building Foundation" or the building exhibits no settlement cracks, deformations, or displacements.	Non-uniform settlement does not exceed the allowable settlement difference specified in the current national standard "Code for the Design of Building Foundation," and the continuous settlement rate of the foundation is less than 2 mm per month for two consecutive months, or although there may be minor cracks in the superstructure, there are no signs of progression.	Non-uniform settlement exceeds the allowable settlement difference specified in the current national standard "Code for the Design of Building Foundation," or the continuous settlement rate of the foundation is greater than 2 mm per month for two consecutive months, or there are settlement cracks in the superstructure wider than 5 mm, and these cracks show no signs of stopping in the short term.	Non-uniform settlement is significantly greater than the allowable settlement difference specified in the current national standard "Code for the Design of Building Foundation," the continuous settlement rate of the foundation is greater than 2 mm per month for two consecutive months, and there is an accelerating trend, or the settlement cracks in the superstructure are noticeably developing, with masonry cracks wider than 10 mm.
Foundation	Foundation Bearing Capacity ( $R/\gamma_0 S$ )	$\geq 1.00$	1.00 to 0.95	0.95 to 0.90	$< 0.90$
	Foundation Damage	No obvious damage, such as corrosion, efflorescence, loosening, peeling, or cracking phenomena.	Minor damage, with slight corrosion, efflorescence, loosening, or peeling occurring in the foundation; or cracks less	Moderate damage, higher than C2 level damage; or cracks wider than 3 mm but not exceeding 10 mm.	Severe damage, with evident corrosion, efflorescence, loosening, or peeling significantly impacting the foundation, or

			than 3 mm wide.		cracks wider than 10 mm.
	Connection Status between Foundation Column Base and Column Footing ( $j_2$ )	0 to 0.05	0.05 to 0.27	0.27 to 0.60	> 0.60
	Foundation Column Displacement ( $j_1$ )	0 to 0.05	0.05 to 0.10	0.10 to 0.17	> 0.17
Beams, Rafters, and Pads (Flexural Members)	Component Deflection /mm	When $h/l > 1/14$ , $\omega_1 \leq l^2/4000h$ . When $h/l \leq 1/14$ , $\omega_1 \leq l/300h$ .	When $h/l > 1/14$ , $l^2/4000h < \omega_1 \leq l^2/3000h$ . When $h/l \leq 1/14$ , $l/400h\omega_1 \leq l/250h$ .	When $h/l > 1/14$ , $l^2/3000h < \omega_1 \leq l^2/2100h$ . When $h/l \leq 1/14$ , $l/250h < \omega_1 \leq l/150h$ .	When $h/l > 1/14$ , $\omega_1 > l^2/2100h$ . When $h/l \leq 1/14$ , $\omega_1 > l/150h$ .
	Component Decay Level	Surface decay or aging deterioration. For $0 \leq \rho_1 < 1/10$ , no heart rot, no knots.	Surface decay or aging deterioration. For $1/10 \leq \rho_1 < 1/7$ , no heart rot; Knot size ratio $m < 1/5$ .	Surface decay or aging deterioration. For $1/7 \leq \rho_1 < 1/5$ , no heart rot; Knot diameter ratio $m < 1/5$ .	Surface decay and aging deterioration rate $\rho_1 < 1/5$ or heart rot $\rho_1 > 1/7$ ; Critical stress location $m < 1/3$ .
	Component Cracks and Width/mm	No cracks.	Cracks present with a slope of 7% to 10%, and the depth of the cracks is not greater than $D/5$ .	Cracks present with a slope of 10% to 15%, and the depth of the cracks is between $D/5$ and $2D/5$ .	Cracks present with a slope greater than 15%, and the depth of the cracks is greater than $2D/5$ .
	Component Connection Status ( $s_2$ )	$< l_0/8$	$l_0/8$ to $l_0/4$	$l_0/4$ to $l_0/2$	$> l_0/2$
Arch Braces	Component Deformation ( $y_1$ )	0 to 0.02	0.02 to 0.04	0.04 to 0.07	$\geq 0.07$
	Component Damage ( $y_2$ )	0 to 0.1	0.1 to 0.2	0.2 to 0.3	$\geq 0.3$
	Component Connection Status ( $s_3$ )	The arches are intact overall, with no signs of depression or displacement.	The arches are in good condition overall, with minor surface cracks but no signs of depression or displacement.	The arch components are all present, with slight displacement in some parts.	Some arch components are missing, with severe depression and significant displacement.



Retaining Walls	Wall Tilt( $q_1$ )	The walls are intact, with no tilting.	The wall tilting is less than H/400.	The wall tilting is less than H/300.	The wall tilting is greater than H/300.
	Wall Weathering ( $q_2$ )	The walls are intact, with no signs of weathering.	The walls show signs of weathering, but no continuous weathered segments exceeding 1 m in length.	The walls show signs of weathering, with continuous weathered segments exceeding 1 m in length and weathering degree $\rho_2 < 1/5$ .	The walls show signs of weathering, with continuous weathered segments exceeding 1 m in length and weathering degree $\rho_2 > 1/5$ .
	Wall Cracks ( $q_3$ )	The walls are intact with no cracks.	The walls are generally in good condition, with minor cracks that do not penetrate through the walls, and there are no cracks at the wall junctions.	The walls have several noticeable cracks, but none are penetrating, and there are no cracks at the wall junctions. Additionally, the cracks are less than 5 mm wide.	The walls have multiple cracks, with at least one crack exceeding half the height of a story, or there are penetrating cracks at the wall junctions, with cracks wider than 5 mm.
Beam-Truss Connection	Repair Frequency	For nationally protected cultural heritage sites such as temples, major repairs are conducted every 10 years; for large palaces, major repairs occur every 40 years.	For nationally protected cultural heritage sites such as temples, major repairs are conducted every 10 to 20 years; for large palaces, major repairs occur every 40 to 60 years.	For nationally protected cultural heritage sites such as temples, major repairs are conducted every 20 to 40 years; for large palaces, major repairs occur every 60 to 80 years.	No repairs have been conducted since the founding of the country.
	Building History	0 to 100	100 to 300	300 to 500	> 500
Roof Structures	Damage to Grey Brick( $k_1$ )	The damage to the grey back is less than 0.01 and there are no exposed rafters.	The damage to the grey back is greater than 0.01 but less than 0.05, and there are no exposed rafters.	The damage to the grey back is greater than 0.05, and there are no exposed rafters.	The damage to the grey back is greater than 0.05 and there are exposed rafters or other wooden structures.
	Tile Integrity( $k_2$ )	0.00 to 0.05	0.05 to 0.10	0.10 to 0.20	> 0.20
	Water Leakage	No	/	/	Yes

Notes:  $l$  is the calculated span of the beam purlin;  $h$  is the height of the column;  $l_0$  is the length of the tenon;  $D$  is the diameter of the column;  $R$  is the column diameter of the column section;  $H$  is the height of the wall.

**Table 2.1.** Meaning of Symbols

No.	Name	Meaning
1	Corrosion ageing deterioration rate $\rho_1$	The ratio of the area of corrosion and ageing deterioration (the sum of both) to the whole cross-sectional area
2	degree of weathering (geology) $\rho_2$	Ratio of average weathering depth of wall to wall thickness
3	Wood knot size ratio $m$	The ratio of the maximum size of the wood knots to the measured circumference of the original part of the log.
4	$j_1$	The ratio of the actual bearing between the ground at the foot of the column and the base of the column to the original cross-sectional area of the column
5	$j_2$	Ratio of column misalignment distance to column diameter
6	$y_1$	Ratio of the area occupied by the cross-section damage to the entire cross-sectional area
7	$y_2$	The overall arch corner in rad.
8	$k_1$	Ratio of damaged grey back to original grey back area
9	$k_2$	Ratio of damaged tile to original tile area

*Qualitative factor evaluation index grading standards*

Due to the unavailability of data on the bearing capacity of building foundations and foundation loads under detection conditions and survey circumstances, a qualitative assessment was conducted. Based on the level of safety, wooden structures in ancient buildings are categorized into four grades. The qualitative factor evaluation index scaling standards for the safety assessment of wooden structures in ancient buildings are established using expert knowledge (see Table 3).

**Table 3.** The Assessment Index Classification Standard for Qualitative Factors

Evaluation Criterion	High	Medium	General	Poor
Score	0.9 to 1	0.8 to 0.9	0.5 to 0.8	0 to 0.5
Foundation Bearing Capacity	$\geq 1.00$	1.00 ~ 0.95	0.95 ~ 0.90	< 0.90
Substructure Bearing Capacity	$\geq 1.00$	1.00 ~ 0.95	0.95 ~ 0.90	< 0.90
Note	Bearing Capacity = $R/r_0S$			

#### *Dimensionless data processing*

The indicators in the established evaluation system possess different dimensions and units. It is challenging to compare them. Hence, the range transformation method was employed to process dimensionless data (Chen *et al.* 2013).

For indicators with a "the larger, the better" orientation:

$$y_{ij} = \frac{x_{ij} - x_{\min(j)}}{x_{\max(j)} - x_{\min(j)}} \quad (5)$$

For indicators with a "the smaller, the better" orientation:

$$y_{ij} = \frac{x_{\max(j)} - x_{ij}}{x_{\max(j)} - x_{\min(j)}} \quad (6)$$

In the equations,  $y_{ij}$  represents the dimensionless processed value,  $x_{ij}$  is the original data,  $x_{\max(j)}$  represents the maximum value in the  $j$ -th row of data, and  $x_{\min(j)}$  is the minimum value in the  $j$ -th row of data. It is also noted that when the control variables are already within the range [0, 1], it is unnecessary to process dimensionless data.

#### *Evaluation rules based on mutation theory*

Data processing is carried out using the normalization formulas corresponding to the mutation types (see Table 1). Scales and grouping values were categorized and determined using recursive operations. Multi-objective mutation evaluation follows the following rules (Li *et al.* 2011):

Complementarity rule: In the system, when control variables (such as  $a$ ,  $b$ ,  $c$ , and  $d$ ) can replace or complement each other, state variables are used as the average of the control variables.

$$x = \frac{x_a + x_b + x_c + x_d}{4} \quad (7)$$

Non-complementarity principle: In the system, when control variables cannot replace or complement each other, state variables are used as the minimum value of the control variables.

$$x = \min \{x_a, x_b, x_c, x_d\} \quad (8)$$

#### *Evaluation grades and significance*

Table 4 shows the safety assessment standards for timber-framed ancient buildings. It was developed upon the analysis of the mutation model for evaluating wooden structures in ancient buildings and the identification of its main factors.

**Table 4.** Safety Evaluation Standards for Wooden Structures in Ancient Buildings

Safety Level	High/I	Medium/II	General/III	Poor/IV
Mutant Grouping Value	0.9 to 1	0.8 to 0.9	0.5 to 0.8	0 to 0.5

*Comprehensive evaluation analysis*

The obtained grouping function values were quantitatively calculated using the normalization formulas based on mutation theory. This process yielded the mutation grade values for the underlying indicators. Following evaluation criteria, the mutation scales values for each level of indicators were calculated layer by layer until the overall mutation grouping function value of the system was obtained. The safety level of wooden structures in ancient buildings was then determined.

**Engineering Case Study**

Zhijia Temple, located in Beijing, was initially constructed in the eighth year of the Zhengtong Era during the early Ming Dynasty (1443 AD). It served as the ancestral temple of Wang Zhen, a eunuch from the Ministry of Rites, who was highly revered by Emperor Yingzong of Ming. During five centuries, Zhijia Temple has witnessed the transitions from the Ming and Qing dynasties to the People's Republic of China. Designated as one of the first national key cultural heritage sites in 1961, Zhijia Temple has a rigorous overall layout, grand scale, and exceptional artistic and cultural significance.

This study evaluated the wooden structural pathology detection, data analysis, and safety monitoring of Zhijia Temple. Specifically, the analysis was conducted on the wooden structure of the Tathagata Hall inside Zhijia Temple. This case study was also used to apply the aforementioned model into the safety assessment of various structural components within wooden ancient buildings.

**Fig. 4.** Point Cloud Image of Tathagata Hall, Zhijia Temple, Beijing

*On-site inspection equipment and data*

The following equipment was employed in the wooden structure detection of the main hall of the Tathagata Hall in Zhihua Temple (see Table 5), and tested with standard DB11/T 2185-2023, T/CECS 714-2020.

**Table 5.** Equipment Used for Wooden Structure Detection in Ancient Buildings

Number	Equipment Used	Purpose of Use	Detection Time
1	FARO/FocusS330/350 Large-Scale 3D Laser Scanner	Scanning of the overall exterior structure of buildings and large Buddha statues.	2022.03-2022.11
2	Scanning and Photographic Auxiliary Equipment	Reference spheres, shading boards, etc.	2022.03-2022.11
3	Wood Impedance Needle Tester (IML RESI-PD500)	Detection of internal wood structure, such as decay, rot, or hollow areas.	2022.08-2022.11
4	Infrared Thermal Imager	Detection of roof leakage.	2022.09.05/2022.10.03
5	Monitoring Sensors	Detection of settlement.	2023.10.01-2023.10.31
6	Hollow Hammer, Metal Detector	Preliminary survey equipment	2022.03-2022.11

A comprehensive examination was conducted on 151 components inside the Tathagata Hall of Zhihua Temple (Table 7). The primary load-bearing elements comprise a) columns (melon-shaped columns, vertical columns, grass-frame columns), b) beams (embracing beams, three-beam structures, five-beam structures, seven-beam structures, overhanging beams, floor beams, corner beams), and c) bracket sets. The secondary load-bearing components include a) purlins (ridge purlins, hip purlins, step purlins), b) pads (shielding pads, arch pads, gold pads, eave pads, ridge pads), and c) lintels (flat lintels, frontal lintels, ridge lintels, gold lintels, interlocking lintels, aligned with purlins lintels).

Other load-bearing components, including invisible wall columns, were excluded from the inspection. Moreover, areas with visual blind spots were not surveyed. The areas of bracket sets were examined together rather than individual counts.

**Fig. 5.** Zhihua Temple 3D laser scanning and impedance analyzer testing

In the survey of the aforementioned components, an impact wrench was used to tap on the components. When there was a hollow sound, non-destructive testing was conducted using an impedance meter. The results of the non-destructive testing are presented in Table 8. In addressing the issue of uneven settlement in the Tathagata Hall of Zhuhua Temple, the uneven settlement sensor parameters are shown in Table 6. Monitoring was conducted at six designated positions (see Fig. 6). Sensor-1 was placed on the south side of the eastern

façade. Sensor-2 was on the east side of the northern façade. Sensor-3 was on the north side of the western facade, and Sensor-4 was on the south side of the western facade. Sensor-5 was placed near the southwest corner next to the water room, and Sensor-6 was in the water room. The data collector was positioned inside the management hall.

Data collection was sampled and completed in October 2023, and the results are summarized in Table 6.1.



**Fig. 6.** Zhihua Temple sensor locations and location of sensor-1

**Table 6.** Sedimentation Sensor Parameters

Parameter	Norm	Parameter	Norm
Range	0-500-2500 mm H <sub>2</sub> O	Response Time	0.2 s
Sensitivity	0.01 mm H <sub>2</sub> O	Output Signal	RS485
Frequency Response Resolution	100 Hz	Average working time	>45000 hours/times
Accuracy	0.01 mm H <sub>2</sub> O	Waterproof rating	IP67
Long-term stability	0.2 mm H <sub>2</sub> O, temperature conditions-45~85°C	Weight	IP671000g
Power-up time	°C<0.51mmH <sub>2</sub> O, temperature conditions-45 to 85°C		

**Table 6.1.** Monitoring Data for Wooden Structure Ancient Building in the Tathagata Hall

Serial Number	Mean Value (mm)	Maximum Value (mm)	Minimum Value (mm)
DIS-G101-01	2.420	4.895	1.369
DIS-G101-02	3.225	5.652	1.119
DIS-G101-03	2.915	5.033	0.702
DIS-G101-04	3.968	6.081	3.025
DIS-G101-05	3.845	5.928	2.948
DIS-G101-06	5.461	30.902	-5.735

**Table 7.** Survey Data for Wooden Structure Ancient Building in the Tathagata Hall

Component Category	Columns		Type Beams Purlins and Rafters			Bracket Arches
	Vertical Column	Cantilever Column	Beams	Component Category	Vertical Column	
Number of Components	22	9	71	21	20	8

**Table 8.** Inspection Data for Wooden Structure Ancient Building in the Tathagata Hall

Component Category	Columns		Type Beams Purlins and Rafters			Bracket Arches
	Vertical Column	Cantilever Column	Beams	Rafters	Purlins Cushions	
Number of Components	14		27	1	6	0

*Evaluation scores for indicators*

In accordance with the wooden structure safety assessment framework (see Fig. 1), a qualitative analysis was applied to assess the bearing capacity of the foundation and base (C1, C3) in the Tathagata Hall of Zhihua Temple. A specialized evaluation panel consisting of three experts in the field and an internal management personnel was established. Qualitative assessments of the indicators were conducted (see Table 3), and the mean of the scores was calculated. Table 10 presents the results of the evaluation for these two indicators rated by the assessment panel.

In addition, data for the quantitative indicators were obtained as shown in Table 9.

**Table 9.** Indicators and access to them

Indicator	Method of data acquisition
Foundation and foundation	monitoring system, status survey
Column	Impedance meter, current survey, point cloud map
Beams, purlins, pads (bending members)	Point cloud diagram, current condition survey, Impedance meter
Arch	Point cloud diagram, current condition survey
Roof structure	Infrared thermal imaging, current survey
Building association	Literature, interviews
Walls	Point cloud diagram, current condition survey

*Wooden structure safety assessment*

A dimensionless processing was applied to each factor in Table 9.1. Equation 6 was utilized for data processing, using indicators C2, C4-C20, C23, and C24 with smaller values, which have a lesser impact on the safety of wooden structures. Differently, Eq. 5 was employed to analyze the indicators with larger values, which indicate lower risks. The final results are detailed in Table 6.

**Table 9.1.** Quantitative Indicator Data and Dimensionless Processing for Wooden Structure Ancient Building in the Tathagata Hall

Objective Layer	Criterion Layer	Index Layer	Measurement Index	Survey Location					Mean Value	Without Dimension
				D	E	F	G	H		
A	A1	B1	C1	/	/	/	/	/	/	/
			C2	2.420mm	3.225mm	2.915 mm	3.968 mm	3.845 mm	3.275 mm	0.4479
		B2	C3	/	/	/	/	/	/	/
			C4	0	2 mm	0	0	0	0.4 mm	0.8
			C5	0	0	0	0	0.02	0.004	0.8
			C6	0	0	0	0	0	0	1.0
	A2	B3	C7	0.1475	0.2025	0.1325	0.075	0.06	0.1235	0.55
			C8	0	0	0	0.075	0	0.015	0.8
			C9	1 cm	0.5 cm	0	0	0	0.3 cm	0.7
		B4	C10	0	0	0	0.065	0	0.013	0.8
			C11	5 mm	8 mm	7 mm	11 mm	6 mm	7.4 mm	0.6
			C12	0	0	0	0.075	0	0.015	0.8
			C13	1 cm	0.5 cm	0	0	0	0.3 cm	0.7
			C14	0	0	0	0.065	0	0.013	0.9
		B5	C15	0	0	0.015	0	0.01	0.005	0.67
			C16	0	0	0.1 mm	0.0	0.0	0.02 mm	0.98
			C17	0	0	0	0.065	0.0	0.013	0.90
	A3	B6	C18	No tilting						1.0
			C19	0	0	0	0	0	0.0	1.0
			C20	0	0	0	0	0	0.0	1.0
		B7	C21	Recently repaired						1.0
			C22	584 years						0.4
		B8	C23	0	0	0	0	0		1.0
			C24	0	0	0	0	0	0.0	1.0
			C25	No leakage					0.11	1.0

**Table 10.** Qualitative Indicator Data and Dimensionless Processing for Wooden Structure Ancient Building in the Tathagata Hall

Objective Layer	Criterion Layer	Index Layer	Measurement Index	Survey Location					Mean Value	Without Dimension
				D	E	F	G	H		
A	A1	B1	C1	0.90	0.80	0.95	0.90	0.90	0.89	0.60
		B2	C3	0.90	0.90	0.95	0.85	0.90	0.90	0.50

The indicator system shows that the components in the butterfly mutation model included: C3, C4, C5, C6, and B2; C7, C8, C9, C10, and B3; C11, C12, C13, C14, and B4. Those forming the swallowtail mutation model included: C15, C16, C17, and B5; C18, C19, C20, and B6; C23, C24, C25, and B8; B3, B4, B5, and A2; B6, B7, B8, and A3; A1, A2, A3, and A. The components constituting the pointed mutation model were: C1, C2, and B1; C21, C22, and B7; B1, B2, and A1. The normalized values of the bottom-level indicators were calculated using the formulas in Table 1. Taking B3 as an example, the calculation process was as follows:

The dimensionless values of the third-level indicators C7, C8, C9, C10 were 0.55, 0.8, 0.7, and 0.8, respectively. Substituting these values into the butterfly-type normalization formula in Eq. 4, and through quantified recursive calculations, the normalized results for the second-level indicators were obtained as follows:



$X_{C7}=\sqrt{0.55}=0.74, X_{C8}=\sqrt[3]{0.8}=0.93, X_{C9}=\sqrt[4]{0.7}=0.91, X_{C10}=\sqrt[5]{0.8}=0.96$ . Using the same method, the normalized values for other indicators at the bottom level were calculated, as shown in Table 11

**Table 11.** Normalized Values of Bottom-Level Indicators for Wooden Structure Ancient Building in the Tathagata

C1	C2	C3	C4	C5	C6	C7	C8	C9	C10	C11	C12	C13
0.77	0.76	0.70	0.93	0.95	1	0.74	0.93	0.91	0.96	0.77	0.93	0.91
C14	C15	C16	C17	C18	C19	C20	C21	C22	C23	C24	C25	
0.98	0.82	0.99	0.97	1	1	1	1	0.74	1	1	1	

The bottom-level control variables in the safety assessment indicators for the wooden structure of the Tathagata Hall in Zhihua Temple were independent with a mutual impact on each other. Equation 7 was used, and the mutation level values for B1 were calculated as follows:  $X_{B1}=\frac{x_{c1}+x_{c2}}{2}=0.765, X_{B2}=\frac{x_{c1}+x_{c2}+x_{c3}+x_{c4}}{4}=0.895$ . Using the same method, the mutation values for each indicator were determined, as outlined in Table 12.

**Table 12.** Normalized Values of Bottom-Level Indicators for Wooden Structure Ancient Building in the Tathagata

Index Layer	B1	B2	B3	B4	B5	B6	B7	B8
Mutation Grouping Function Value	0.765	0.895	0.885	0.897	0.927	1	0.870	1
Criterion Layer	A1		A2		A3			
First-level Mutation Membership Function Value	0.919		0.962		0.990			
Objective Layer	A							
Total Mutation Membership Function	0.987							
Safety Level	Level I							

*Wooden structure safety assessment*

The total mutation grouping function value ( $X_A$ ) derived from the mutation theory was determined as 0.987, corresponding to Scale I rating. This indicates a high safety level for the wooden structure of the Tathagata Hall in Zhihua Temple. It was noted that this result aligns with assessments obtained through other methods such as Analytic Hierarchy Process (AHP) and Fuzzy Mathematics (see Table 13) (Guo *et al.* 2017; Wang *et al.* 2022).

**Table 13.** Comparative Analysis of Ancient Building Wooden Structure Safety Assessment Methods Results

Project	Document (Guo <i>et al.</i> 2017)	Document (Wang <i>et al.</i> 2022)	This Study
Evaluation Method	Grey Whitening Weighted Function Clustering Method	Matter-element Model	Mutation Theory
Safety Level	High	High	High
Evaluation Scale	Level I	Level I	Level I

## RESULTS AND DISCUSSION

Table 9 presents that the total mutation degree ( $X_A$ ) for the main hall of Zhihua Temple is 0.987, corresponding to a high safety level. The sub-level mutation degrees ( $X_{A1} = 0.919$ ,  $X_{A2} = 0.962$ ,  $X_{A3} = 0.990$ ) of individual components also fall within Level I. Particularly, the roof maintenance structure aligns with the actual on-site conditions, as it has recently undergone rigorous repairs.

The value of  $X_{B1}$  was calculated as 0.765, indicating that the primary factors influencing the safety of B1 are foundation bearing capacity and uneven settlement. The safety level of B1 was at Level III. The analysis of the monitoring data for the entire month of October 2023 reveals ongoing uneven settlement, with the highest value reaching 6.081 mm. Therefore, a high level of attention, supervision, and control over internal visitor traffic is essential.

According to the available data,  $X_{B2} = 0.895$ ,  $X_{B3} = 0.885$ , and  $X_{B4} = 0.897$ . Currently, the safety levels of B2, B3, and B4 are at Level II. The potential influencing factors for B2 include foundation bearing capacity, as indicated by the normalized value  $X_{C3} = 0.7$  for C3. For B3, the influencing factor is the degree of column deflection ( $X_{C7} = 0.74$  for C7); and for B4, it is the component deflection ( $X_{C11} = 0.77$  for C11). The observed indicators are given significant attention, with strengthened supervision recommended.

## CONCLUSIONS

1. An evaluation model based on mutation theory was established by analysing the characteristics of wooden structures and the factors affecting the safety of wooden ancient buildings. The model considered 3 aspects, namely the foundation, upper load-bearing structure, and maintenance structure level association, *etc.*, with 2 qualitative and 23 quantitative bottom indicators. The quantitative indicators were determined by scientific testing means to determine the raw data of the indicators, and the data were transformed into quantitative data of the indicators through standard norms, while the qualitative indicators were determined by a number of experts by assigning scores and seeking the average of the scores according to the actual situation, so as to achieve unification of the quantitative standards of the qualitative and quantitative indicators. The quantitative and qualitative indicators are unified.
2. The safety evaluation model based on mutation theory of wood structure ancient buildings established was applied in examples, and the evaluation results were basically consistent with the results of the grey fuzzy theory evaluation using other safety evaluation methods of wood structure ancient buildings. These findings showed that the method is feasible. On the basis of the evaluation results, corresponding risk prevention and control measures can be scientifically formulated.
3. For the first time, the mutation theory has been introduced into the safety assessment of wooden structures of ancient buildings, which has certain superiority compared with other assessment methods. Firstly, the evaluation method is to some extent more suitable for the characteristics of the damage of wooden buildings than other safety assessment methods for wooden buildings; secondly, a model for safety assessment of wooden buildings was established based on the mutation theory, which avoids subjectivity in the selection of assessment indexes and determination of the weights of

the indexes; and then, the ratio of the quantitative indexes to the qualitative indexes and the acquisition of the indexes are more suitable than other assessment methods for the safety assessment of wooden buildings. Then, in terms of the proportion of quantitative and qualitative indicators and the acquisition of indicator data, the model has been greatly improved compared with other studies on the safety assessment of wood-framed ancient buildings, which improves the objectivity of the whole safety assessment; finally, the calculation of the mutation theory model of wood-framed ancient buildings is simpler than other assessment models, with a small amount of calculations that are simple and easy to carry out, which makes the model better and more efficient in the wood-framed ancient building protection surveys.

## ACKNOWLEDGMENTS

The study was supported by the Beijing Natural Science Foundation (No. 8232006), the National Natural Science Foundation of China (No. 52278472), and the Beijing Natural Science Foundation (No. 8232004).

## REFERENCES CITED

- Abrahamyan, A. S., Sahakyan, K. G., and Chilingaryan, R. Yu. (2023). "Application of the catastrophe theory to acoustoplasma research," *Journal of Physics: Conference Series* 2657(1). DOI: 10.1088/1742-6596/2657/1/012020.
- Chen, J., Luo, Z., and Hou, Z. (2013). "Stability evaluation of metal mine goaf based on improved mutation series method," *China Production Safety Science and Technology (CPSST)* 9(11), 17-24. (In Chinese) DOI: 10.11731/j.issn.1673-193x.2013.11.003
- Cointe, A., Castera, P., and Galimard, P. (2007). "Diagnosis and monitoring of timber buildings of cultural heritage," *Structural Safety* 29, 337-348. (In Chinese) DOI: 10.1016/J.STRUSAFE.2006.07.013
- DB11/T 2185-2023. "Technical specification for site investigation of wooden structures of ancient buildings," Beijing Municipal Administration of Market Supervision, Beijing, China, in Chinese.
- Gao, B., and Wei, S. (2023). "Evaluation of fire danger level of an ancient building based on mutation level method," *Safety and Environmental Engineering* 30(3), 45-50. (In Chinese) DOI: 10.13578/j.cnki.issn.1671-1556.20210809
- Garziera, R., Amabili, M., and Collini, L. (2008). "Health status of ancient buildings: Interferometric radar ND'T inspection," *Physiopraxis* 7(03), 43-45.
- GB/T 50023 (2009). "Standard for seismic appraisal of buildings," Ministry of Housing and Urban-Rural Development of the People's Republic of China (MOHURD), China Architecture and Building Press, Beijing, China, in Chinese.
- GB/T 50165 (1993). "Technical code for maintenance and strengthening of ancient timber buildings," Ministry of Housing and Urban-rural Development of the People's Republic of China (MOHURD), China Architecture and Building Press, Beijing, China, in Chinese.

- GB/T 50292 (2016). "Standard for appraisal of reliability of civil buildings," Ministry of Housing and Urban-rural Development of the People's Republic of China (MOHURD), China Architecture and Building Press, Beijing, China, in Chinese.
- Gu, H. (2009). *Reliability Assessment of Brick and Stone Ancient Pagodas Based on Fuzzy Synthetic Evaluation Theory*, Master's Thesis, Beijing Jiaotong University, Beijing, China.
- Guo, X., Ti, F., and Xu, S. (2017). "Safety assessment of wooden ancient buildings based on grey whitening weight function clustering method," *Journal of Beijing University of Technology* 43(5), 6. (In Chinese) DOI: 10.11936/bjtxb2016060034
- Guo, X., Xu, S., Song, X., and Wang, Y. (2016). "Safety assessment of ancient timber buildings based on gray-fuzzy analytical method," *Journal of Beijing University of Technology* 42(3), 393-398. (In Chinese) DOI: 10.11936/bjtxb2015040074
- Huan, J., Ma, D., Wang, W., and Wang, Z. (2019). "Safety state evaluation method based on attribute recognition model for ancient timber buildings," *Advances in Civil Engineering* 2019, 1-13. Article ID 3612535. DOI: 10.1155/2019/3612535
- Jiang, A., Dong, Y., and Liu, J. (2020). "Research on construction risk prediction model of metro station based on mutation level method," *Journal of Safety and Environment* 20(3), 832-839. (In Chinese) DOI: 10.13637/i.issn.1009-6094.2019.0338
- Kang, L. (2014). *Research on the Safety Assessment Method of Pipeline in Coal Mining Airspace Area*, Master's Thesis, Southwest Petroleum University, Cheng du, China. (In Chinese)
- Li, C., Fang, J., He, Z., and Mao, W. (2011). "Research on safety management evaluation of construction enterprises based on mutation theory," *China Production Safety Science and Technology (CPSST)* 7(12), 87-91. (In Chinese) DOI: 10.3969/j.issn.1673-193X.2011.12.015
- Li, D. (2023). *Research on Safety Risk Assessment of Highway Bridge Construction Based on Fuzzy Catastrophe Theory*, Master's Thesis, Nanhua University, Hunan, China. (In Chinese)
- Li, M. (2021). *Fire Risk Assessment of High-Rise Civil Buildings Based on Catastrophe Theory*, Master's Thesis, Chongqing University, Chongqing, China. (In Chinese)
- Liang, S. (2005). *History of Chinese Architecture*, Baihua Wenyi Press, Tianjin, China. (In Chinese)
- Lima, H. F., Vicente, R., Nogueira, R. N., Abe, I., Andre, P., Fernandes, C., Rodrigues, H., Varum, H., Kalinowski, H., Costa, A., et al. (2018). "Structural health monitoring of the church of Santa Casa da Misericordia of Aveiro using FBG sensors," *IEEE Sensors Journal* 8(07), 1236-1242. DOI: 10.1109/JSEN.2008.926177
- Ling, F. (1987). *Mutation Theory and its Application*, Shanghai Jiaotong University Press, Shanghai, China. (In Chinese)
- Luo, G., Qi, Y., and Liang, S., Luo, J., and Jia, C. (2020). "Safety assessment method of load-bearing wooden frames of ancient buildings based on BP algorithm," in: *Industrial Buildings Symposium*, Beijing, China. (In Chinese) DOI: 10.26914/c.cnkihy.2020.024533
- Ma, B. (2007). "Examining the special patterns of conservation and restoration of chinese cultural heritage ancient buildings through the practice of maintenance and protection of temples for emperors throughout dynasties," *Proceedings of the China Forbidden City Society* 5, 37-56. (In Chinese)
- Pan, Y., Li, L., Wang, H., and Yao, Y. (2016). "Study on post-earthquake damage assessment methods for wooden traditional buildings," *Journal of Hunan University*

- (*Natural Sciences*) 43(1), 132-142. (In Chinese) DOI: 10.16339/i.cnki.hdxzbzkb.2016.01.018
- Qin, B., Li, Q., and Tan, J. (2017). "Safety evaluation of masonry and wooden structure ancient buildings based on fuzzy hierarchical analysis approach," *Journal of Civil Engineering and Management* 34(5), 52-59. (In Chinese) DOI: 10.13579/j.cnki.2095-0985.2017.05.009
- Shu, C., Yao, A., Xu, T., Wang, H., and Qin, C. (2017). "Study on the evaluation of gas pipeline hazard in the mining collapse area based on mutation theory," *China Production Safety Science and Technology (CPSST)* 13(1), 97-102. (In Chinese) DOI: 10.11731/j.issn.1673-193x.2017.01.016
- Stamovlasis, D., Giannouli, V., Vaiopoulou, J., and Tsolaki, M. (2022). "Catastrophe theory applied to neuropsychological data: Nonlinear effects of depression on financial capacity in amnesic mild cognitive impairment and dementia," *Entropy* 24(8), 1089-1089. DOI: 10.3390/E24081089
- T/CECS 714-2020. "Ancient architecture wooden structure inspection technical standards," China Engineering Construction Standardisation Association, China Construction Industry Press, Beijing, China, in Chinese.
- Wang, F., Tan, Z., Zhang, J., and Zhang, R., and Wang, W. (2022). "Research on health diagnosis and safety evaluation of wooden structures of ancient buildings based on object-element modelling," *Forest Industry* 59(3), 55-60. (In Chinese) DOI: 10.19531/j.issn1001-5299.202203010
- Wang, S. (2020). *Research on the Safety Evaluation Method of Brick and Wood Structure Ancient Buildings*, Master's Thesis, Lanzhou University of Technology, Lan Zhou, China. (In Chinese)
- Xu, S., Guo, X., Huang, R., Wang, Y., and Fu, T. (2017). "Safety assessment of ancient timber buildings based on analytical hierarchy process," *Industrial Construction* 46(12), 180-183. (In Chinese) DOI: 10.13204/j.gyjz201612034
- Zhang, G., and Zhang, R. (2017). "Lifetime prediction of Huizhou ancient buildings based on improved Elman neural network," *Journal of the University of Science and Technology of China* 47(10), 817-822. (In Chinese) DOI: 10.3969/i.issn.0253-2778.2017.10.003
- Zhou, Z. (1989). *Rehlertom. Mutationism: Ideas and Applications*, Translated version, Shanghai Translation Publishing House, Shanghai, China.
- Zhu, J., and Li, T. (2020). "Catastrophe theory-based risk evaluation model for water and mud inrush and its application in karst tunnels," *Journal of Central South University: Science and Technology of Mining and Metallurgy* 27(23), 1587-1598. DOI: 10.1007/s11771-020-4392-0

Article submitted: March 18, 2024; Peer review completed: June 8, 2024; Revised version received and accepted: July 14, 2024; Published: July 28, 2024.

DOI: 10.15376/biores.19.3.6690-6710